CONSTRAINING THE CONTEMPORARY IMPACT CRATERING RATE AND UNDERSTANDING THE IMPACT PROCESS WITH TEMPORAL AND PHOTOMETRIC OBSERVATIONS. E. J. Speyerer[1], R. V. Wagner[1], R. Z. Povilaitis[1], M. S. Robinson[1], A. C. Martin[1], A. Boyd[1], and B. W. Denevi[2], [1]Arizona State University, School of Earth and Space Exploration, Tempe, AZ, (espeyerer@ser.asu.edu), [2]Johns Hopkins University Applied Physics Laboratory, Laurel, MD, USA

Introduction: Lunar Reconnaissance Orbiter Camera (LROC) observations are key in examining the recent impact flux and the results of the impact process itself. With more than a decade of meter-scale mapping, over 500 newly formed impact craters have been discovered, measured, and in some cases dated to within a month of their formation. As the temporal baseline increases throughout Extended Science Mission 4 (ESM4), we will continue to refine the contemporary cratering rate and compare the impact frequency to Mars and other planetary bodies. Furthermore, follow-up observations of the impact site under a variety of lighting and viewing geometries aids us in understanding the spectral and photometric properties surrounding the impact site.

Temporal Imaging & Impact Identification: Since 2009, the twin Narrow Angle Cameras (NACs) and Wide Angle Camera (WAC) [1] have collectively captured over 1,690,000 and 393,000 images, respectively, of illuminated Moon. Using a subset of NAC images (50-150 cm pixel scale), we analyzed tens of thousands of before and after temporal image pairs that cover the same spatial area with similar lighting (incidence angle difference < 3°). From the search, we located newly formed craters down to the limit of resolution (~1.5 m), secondary impacts, rock falls, and recent mass wasting events [2,3].

To identify larger impacts (up to 100 m) that occur less frequently, we compared temporal observations with the WAC. To pinpoint these sub-pixel sized impact events, the signal to noise ratio was improved by combining multiple band and/or images together. Using the first method, each of the five visible bands were map projected, and then spatial filters were used to match the intensity across all the visible bands. The bands were later merged into a single image using median filtering. This process was repeated for a set of observations acquired later in the mission, and the two composite mosaics were then manually compared to locate large impacts.

Alternatively, stacks of observations were combined to make composite images. Instead of combining the individual bands, the composite was created by merging tens of individual WAC observations collected over a series of months of the same region. These composite products were also compared to similar composites made from observations acquired later in the mission. Both methods successfully identified larger impacts that have yet to be captured in NAC temporal imaging (note: only ~20% of the Moon is covered in NAC temporal images). The latter method had high enough SNR to identify distal low reflectance zones around craters as small as 10 m in diameter. Studying additional NAC and WAC observations and temporal images gathered in ESM4 will enable further refinement of the contemporary crater size frequency distribution (CSFD) (**Fig. 1**).

To provide additional constraints on the cratering rate, we are currently analyzing temporal images using Apollo Metric and Kaguya Terrain Camera images as the before images and LROC observations for the after comparison. Even with the coarser resolution, the extended baseline makes it possible to identify large craters (~100 m), which are not as well represented in the contemporary CSFD.

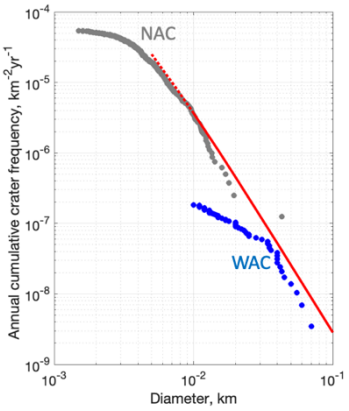

Fig. 1- Annual cumulative crater frequency observed with the LROC NAC (gray) and LROC WAC (blue). The red line is a 1-year isochron derived using Neukum et al. 2001 estimates [4]. The current counts indicate a slightly steeper contemporary production rate as opposed to the shallower rate observed on Mars.

Newly formed impacts: Temporal image ratios of the before and after images reveal up to 4 reflectance zones around the new impact craters [1, 4]:

- Proximal high reflectance zone (PHRZ)
- Proximal low reflectance zone (PLRZ)
- Distal high reflectance zone (DHRZ)
- Distal low reflectance zone (DLRZ)

These changes in the surface reflectance are caused by exposure of immature regolith as well as changes in the regolith properties. By merging multiple WAC observations, faint distal zones (1-2% decrease in surface reflectance) can be seen over a thousand crater diameters away from the impact site. To examine color variations, each of the WAC spectral bands were merged separately and seven (321 to 689 nm; two ultraviolet and five visible) temporal ratios were constructed. To date, we have not identified any significant color variation in

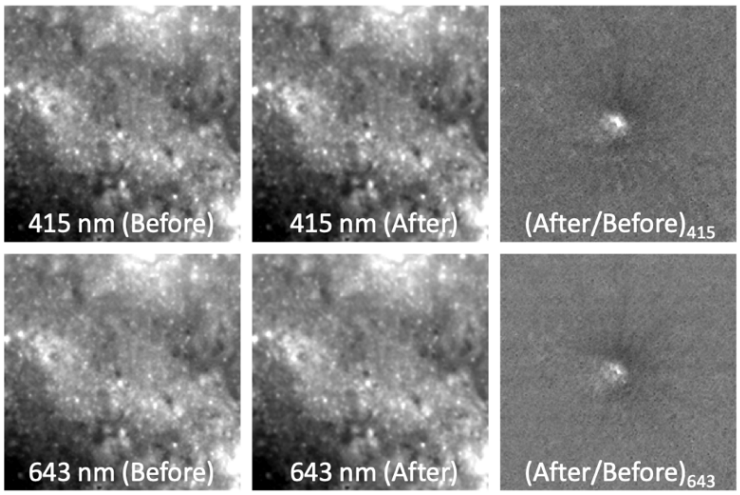

Fig. 2- LROC WAC temporal observations of a new 43 m crater. The third column shows the traditional temporal ratios constructed from two WAC bands (415 and 643 nm). The last column is a ratio of the temporal ratios highlighting changes in the spectral slope associated with the impact event. Each frame is 20 km across.

the distal reflectance zones. However, we do see color variation in the proximal zones (**Fig. 2**).

From these multispectral observations, we infer that the proximal zone is exposing immature regolith that is indicated by bluer slope in the band ratio (**Fig 2**). Meanwhile the lack of change in the band ratio covering the distal zones indicates that its formation is not the result of the deposition of a darker or brighter material, but rather a local effect that is altering the photometric properties.

Photometric Observations: As new impacts are discovered, follow-up NAC observations are acquired over a range of lighting and viewing geometries. Photometric image sequences can be constructed from these observations spanning many years to study how the surface reflectance varies spatially and temporally and to infer properties of the regolith. For one newly formed 50 m crater, we have acquired twenty NAC observations with phase angles ranging from 1.5 to 88 degrees. Based on analysis of these image sequences, we infer that the PHRZ, located closest to the crater rim, has lower porosity. This may be due to the emplacement of small rocks, an increase in the relative grain size, and/or compaction of the surface based on the shallower slope of the phase curve near opposition (**Fig. 2c**). Meanwhile, we infer that the adjacent PLRZ has higher porosity (than the background regolith), possibly due to fewer rocks, a decrease in the relative grain size, and/or dilation of the surface based on a steeper slope near opposition. Meanwhile, at larger phase angles (40-80°), the difference in the two proximal zones seen in **Fig. 2c** disappears (**Fig. 2d**). This indicates that the sub-pixel roughness increases in both proximal zones compared to the background and is consistent with current cratering models.

For larger impacts (Diam. > 30 m), most of the distal zones and several of the proximal zones can be interrogated using WAC observations. Each month, the WAC (with its 60 degree field of view) observes the impact site under a different lighting and viewing geometry even without a slewed observation. From this dataset, the shape of the phase curve can be estimated for much broader regions than can be achieved with NAC temporal imaging. When analyzing a newly formed 70 m crater at phase angles < 30°, the DHRZ has a higher reflectance than before the impact, but the difference nearly inverts at phase angles > 60°. Meanwhile, the DLRZ is suppressed across the entire phase range investigated and shows signs of increased backscatter.

References: [1] Robinson M. S. et al. (2010) *Space Sci. Rev.*, 150, 81–124. [2] Speyerer E. J., et al (2016) *Nature*, 538, 215-218 [3] Robinson M. S. et al. (2015) *Icarus*, 252, 229-235. [4] Neukum et al. (2001) *Space Science Reviews* 96, 55-86.

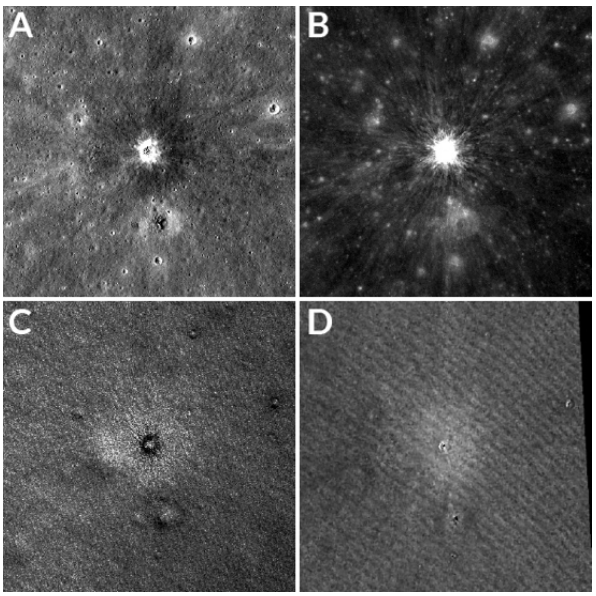

Fig. 3- A and B) Set of after images acquired at 65° and 2° phase, respectively. C and D) Phase ratio images of NAC observations C) 2°/7° D) 52°/79°.